Magnetic Raman Scattering from 1D Antiferromagnets

Rajiv R. P. Singh,[1] Peter Prelovšek,[2,3,4] and B. Sriram Shastry[5,4]

[1]*Department of Physics, University of California, Davis, California 95616*
[2]*Max-Planck-Institut für Festkörperforschung, Heisenbergstrasse 1, D-70569 Stuttgart, Germany*
[3]*J. Stefan Institute and Department of Physics, University of Ljubljana, 1001 Ljubljana, Slovenia*
[4]*Institute of Theoretical Physics, Santa Barbara, California 93106*
[5]*Indian Institute of Science, Bangalore, India 560012*

We study Raman scattering from 1D antiferromagnets within the Fleury-Loudon scheme by applying a finite temperature Lanczos method to a 1D spin-half Heisenberg model with nearest-neighbor (J_1) and second-neighbor (J_2) interactions. The low-temperature spectra are analyzed in terms of the known elementary excitations of the system for $J_2 = 0$ and $J_2 = 1/2$. We find that the low-T Raman spectra are very broad for $|J_2/J_1| \lesssim 0.3$. This broad peak gradually diminishes and shifts with temperature, so that at $T > J_1$ the spectra are narrower and peaked at low frequencies. The experimental spectra for $CuGeO_3$ are discussed in light of our calculations.   [S0031-9007(96)01579-7]

Recently there has been much interest in antiferromagnetism and spin-Peierls transition in the quasi-1D material $CuGeO_3$ [1]. These materials exhibit a spin-Peierls transition at $T_{SP} = 14$ K. Above this temperature they are believed to be well described by a quasi-1D Heisenberg model. The temperature dependence of the spin gap below T_{SP} and the spin-wave spectra have been measured in neutron scattering [2,3]. Understanding these experiments have led various theoretical groups to consider a quasi-1D frustrated Heisenberg model with nearest- and second-neighbor antiferromagnetic interactions along the chains [4,5]. It is well known that in the absence of second-neighbor interactions, the ground state has no long range order and spin-spin correlations decay as a power law. With sufficiently large second-neighbor interactions, the ground state spontaneously dimerizes and the spin-excitation spectrum becomes gapped [6].

More recently Raman scattering has also been measured in these systems, independently by different groups [7,8]. Below the spin-Peierls transition, a complete understanding of Raman scattering necessarily requires considerations of phonons and electron-phonon couplings. Here we will concentrate on the experimental spectra above T_{SP}. This spectra appears predominantly with incoming and outgoing light polarized along the *c axis,* the direction of largest exchange couplings in these materials. It is found that the low-temperature spectra are very broad with much of the spectral weight between 200 and 400 cm^{-1}. As the temperature is increased this peak diminishes and is negligible above 80 K, while a much narrower peak appears at low frequencies which grows as the temperature is raised.

The aim of this study is a theoretical understanding of Raman scattering from 1D antiferromagnets. While our primary focus here is on the material $CuGeO_3$, our results should be relevant to understanding magnetic Raman spectra in other quasi-1D antiferromagnets as well. For $CuGeO_3$, one important aspect of Raman scattering is that

it presents an alternative probe and these spectra could lead to establishing the proper model, being controversial so far mainly with respect to the importance of next-neighbor spin interactions. The observed T variation also presents a challenge, since the transformation of broad spectra into a narrow central-peak-like structure at high T is against usual experience of spectra becoming more incoherent and wider with increasing T.

We study the magnetic Raman scattering in these materials within the Fleury-Loudon scheme [9], a formal derivation for which has recently been given by Shastry and Shraiman [10]. To explain the dominant light scattering with incident and outgoing light polarized along the c axis as observed experimentally, one has to go beyond the usually discussed Heisenberg model with nearest-neighbor (J_1) spin interaction. Hence we consider a 1D spin-half Heisenberg Hamiltonian

$$\mathcal{H} = J_1 \sum_i \mathbf{S}_i \cdot \mathbf{S}_{i+1} + J_2 \sum_i \mathbf{S}_i \cdot \mathbf{S}_{i+2}, \qquad (1)$$

including also the next-neighbor (J_2) exchange. If we had purely nearest-neighbor interactions, then there would be no scattering within the Fleury-Loudon scheme as the scattering operator would be proportional to the original Hamiltonian. However "photon assisted superexchange" as in Ref. [10] would give a second-neighbor term in the light scattering Hamiltonian.

Within the space of nearest and next-nearest interactions, an effective Raman operator can be derived, including again both terms, however, with different weights. Since one can always subtract the part commuting with $\mathcal{H}$, without loss of generality, we choose the operator with purely second-neighbor interaction,

$$R = A \sum_i \mathbf{S}_i \cdot \mathbf{S}_{i+2}. \qquad (2)$$

Below the spin-Peierls transition additional staggered terms arise in the Hamiltonian. Then, nearest- and

second-neighbor Raman operators can be distinguished and their relative weights can be addressed.

The Raman spectral function is then given by

$$I(\omega) = \frac{1}{\pi NZ} \text{Re} \int_0^\infty dt\, e^{i\omega t}\, \text{Tr}[e^{-\beta\mathcal{H}} R(t)R(0)], \quad (3)$$

where Z is the partition function. We calculate $I(\omega)$ at finite T (as well as $T = 0$) by studying short chains (with periodic boundary consitions) with up to $N = 24$ spins. Here we employ the finite-T method for dynamic and static correlation functions, based on the Lanczos iteration combined with random sampling [11]. This method has already been used to study several dynamical response functions for the t-J model (as relevant for the cuprates), including the Raman response [12]. In the present calculations we use $M_0 = 100-150$ Lanczos steps and random sampling over $N_0 \sim 600$ initial wave functions. The results are checked on smaller systems by full diagonalization.

As discussed extensively in connection with previous applications, the spectra for small systems reveal macroscopic behavior at finite $T > T^*$, where T^* is related to the low-energy level spacing and is thus dependent on the system size. For the model (1) low-energy gaps are quite substantial (in contrast to the 2D results in Refs. [11,12]), i.e., $T^* \sim 0.4J_1$ for systems considered. At $T < T^*$ we have to add an appreciable broadening Δ to smooth out finite-size dependent peaks in $I(\omega)$.

First let us discuss the variation of the calculated low-T spectra with different J_2, as presented in Fig. 1 for fixed $T = 0.2J_1 \approx 0$ and $-0.5 \leq J_2/J_1 \leq 0.5$. Analogous information can be gained also from the behavior of the frequency moments, which converge more rapidly for finite systems. In Fig. 2 we present $T = 0$ results for the total Raman scattering intensity I_0, the average frequency $\langle\omega\rangle$, and the spectral width σ, all calculated with respect to $I(\omega > 0)$ for systems with $N = 20, 24$.

We find that the low-T spectra show a broad but pronounced peak for small $|J_2/J_1| \lesssim 0.3$. In this parameter range, the peak position shifts a little towards lower energies with increasing J_2. Also, the peak becomes more pronounced for larger J_2. For $J_2 > 0.3J_1$, the spectra change quite dramatically. For $J_2 = J_1/2$, where the ground state is rigorously known to be spontaneously dimerized [6], the peak moves to much lower frequencies, occurring below J_1.

One can get some understanding of these spectra in terms of the elementary excitations of the system, which are well known for $J_2 = 0$. In this case, the elementary excitations are domain walls or spinons with dispersion

$$\epsilon(q) = \frac{\pi J}{2}|\sin q|. \quad (4)$$

Light scattering leads to total spin-zero excitations with total momentum $k = 0$. These can be two- or four-spinon excitations. However, there is vanishing spectral weight for two spinons at $k = 0$. Thus the spectra consist of four-spinon excitations with $k = 0$. These can also be thought of as two magnons with opposite momenta, each of which is a composite of two spinons. Thus the spectra reflect the two-magnon density of states, appropriately weighted by a squared matrix element of the scattering Hamiltonian [13,14]. It is known [15,16] that to get a good description of the dynamic structure factor $S(Q, \omega)$ in terms of noninteracting spinons, the decomposition of magnons with momentum Q in terms of spinons with momenta q and $Q - q$ needs to include extra form factors $\alpha(q, Q - q)$. Specifically, at $T = 0$

$$S_Q^z \sim -i \sum_{0<q<Q} \alpha(q, Q - q)b_q^\dagger b_{Q-q}^\dagger, \quad (5)$$

FIG. 1. Raman intensity I/A^2 vs ω/J_1 for the Heisenberg model with various J_2/J_1, as calculated for fixed $T = 0.2J_1$ and $N = 20$. An additional smoothening with $\Delta = 0.3J_1$ (for $J_2/J_1 = 0, 0.2$) and $\Delta = 0.4J_1$ (other J_2/J_1) is introduced.
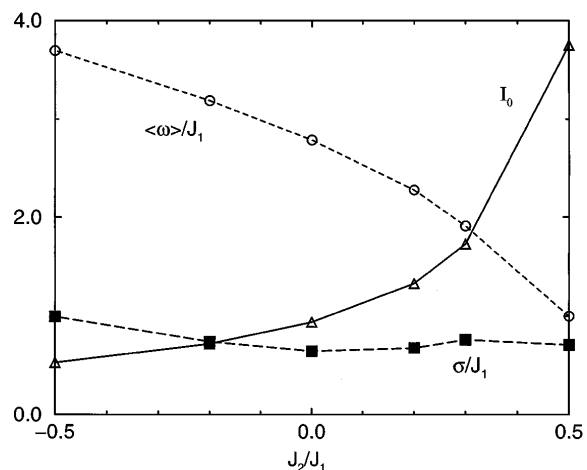
FIG. 2. Total Raman intensity I_0 (arbitrary units), the average frequency $\langle\omega\rangle/J_1$, and the spectral width σ/J_1 vs J_2/J_1 at $T = 0$, as evaluated for systems with $N = 24$ ($J_2/J_1 = 0, 0.2$) and $N = 20$ (other J_2/J_1), respectively.

where S_Q^z is a spin operator, $b_q^\dagger$ represent fermion creation operators for the spinons, and

$$\alpha^2(q, Q - q) = C \frac{|\sin(Q/2 - q)|}{\sqrt{\sin q}\sqrt{\sin(Q - q)}}. \tag{6}$$

This decomposition is not a formal operator identity, but may be regarded as a leading term in a spinon expansion. We can use this to compute the Raman spectral function in Eq. (3) provided we neglect "vertex corrections," which are hard to quantify at present. With this further approximation the Raman spectra can be estimated as

$$I(\omega) = \int_0^\pi dQ \int_0^Q dq_1 \int_0^Q dq_2 \alpha^2(q_1, Q - q_1)\alpha^2(q_2, Q - q_2)$$
$$\times |M_Q|^2 \delta(\omega - \epsilon(q_1) - \epsilon(Q - q_1) - \epsilon(q_2) - \epsilon(Q - q_2)), \tag{7}$$

where $|M_Q|^2$ represents the matrix elements of the Raman operator.

In Fig. 3, we show the spectra $I(\omega)$ evaluated numerically for M_Q equal to 1, $\cos Q$, $\cos 2Q$, and $\cos Q/2$, respectively. The peak in the density of states at $\omega = \pi$ reflects the deCloizeaux-Pearson modes. If the spin waves were well defined excitations, their density of states would diverge at $\pi J/2$, causing a divergence at πJ for two magnons. In reality, these modes are only the bottom of a continuum; nevertheless, a divergent spectral weight at this lower end of the continuum leads to a peak in the two-magnon density of states. This clearly arises from magnons at $Q = \pi/2$ and is thus killed by $M_Q = \cos Q$. The numerical results are consistent with such a peak, although the finite-size effects prevent us from locating it precisely.

On the other hand, the above spinon spectra with $M_Q = \cos 2Q$, as expected for the second-neighbor Raman operator, is inconsistent with the numerical results at low frequencies. Numerical results clearly show that there is very little scattering at low frequencies. Looking at the finite-size effects, we find that the lower end of the spectra scales with size N as $1/N$ but the spectral weight scales as $1/N^3$. This suggests that in the thermodynamic limit, the low frequency spectra scale as ω^3. This discrepancy with
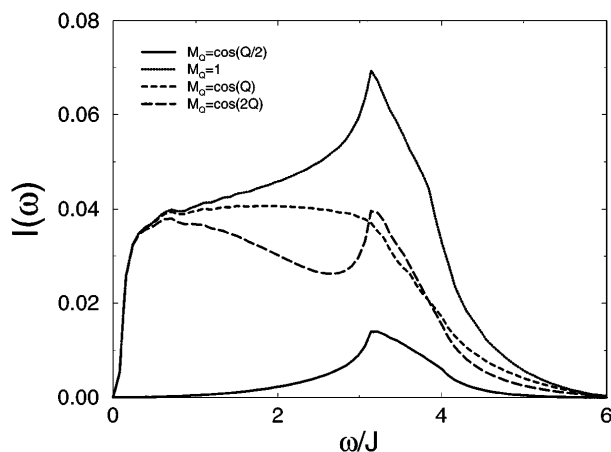
the above spinon estimate is presumably due to the vertex corrections, which must somehow cancel the excessive low-frequency scattering. This result is phenomenologically consistent with $M_Q = \cos Q/2$, which eliminates the low-frequency spectral weight, occurring at $Q = \pi$ [7].

In contrast to the power-law Néel phase, in the spontaneously dimerized phase at larger J_2/J_1 the excitations can be considered as local triplets. A simple estimate of excitation energies in terms of pairs of local triplets would lead to scattering up to $2J_1$. A more careful treatment of the excitations by Shastry and Sutherland [17] suggests that the elementary excitations in this phase are defects, analogous to spinons in the power-law phase. However, there is a gap in the defect excitation spectra; thus, for a defect pair there is finite spectral weight at $Q = 0$. Thus the Raman spectra consist of both two-defect and four-defect components. This leads to an onset in the spectra at about $1/4J_1$ and they extend up to about $2.5J_1$. These features are clearly consistent with our numerical results. The $T = 0$ gaps are found to be $0.345J_1$, $0.30J_1$, and $0.28J_1$ for $N = 16, 20$, and 24, respectively.

Let us now discuss a comparison of calculated spectra with the experimental spectra in CuGeO$_3$ at low $T > T_{SP}$. It is evident that the spectra are inconsistent with $J_2 = 0$ and $J_1 = 80$ K and also with $J_2/J_1 = 0.5$ with $J_1 = 150$ K. The values of $J_1 = 150$ K and $J_2/J_1 \approx 0.2-0.3$ are closest in the peak position and width to the experimental spectra. The spectral shape is somewhat affected by the presence of phonon modes. However, the reported data of both van Loosdrecht et al. and Lemmens et al. seem to have multiple peaks. Our spinon calculation suggests that the main peak should be at twice the maximum energy for single magnons. Neutron scattering [2] shows a maximum in the spin-wave energy at 16.3 meV = 131 cm^{-1}. This translates into a peak in Raman scattering at 262 cm^{-1}. The data are consistent with this result. We have also verified that adding a nearest-neighbor alternating term to our Hamiltonian or to the Raman operator causes a mixing of states with $k = 0$ and $k = \pi$ and leads to Raman scattering at much lower energies. This leads to results consistent with the 30 cm^{-1} peak seen below T_{SP} [8].

In Fig. 4 we present results for the T variation of spectra at fixed $J_2/J_1 = 0.2$. We notice that the low-T

FIG. 3. The density of states for four spinons evaluated with matrix elements $M_Q = 1$, $\cos Q$, $\cos 2Q$, and $\cos Q/2$, respectively [see Eq. (7)].
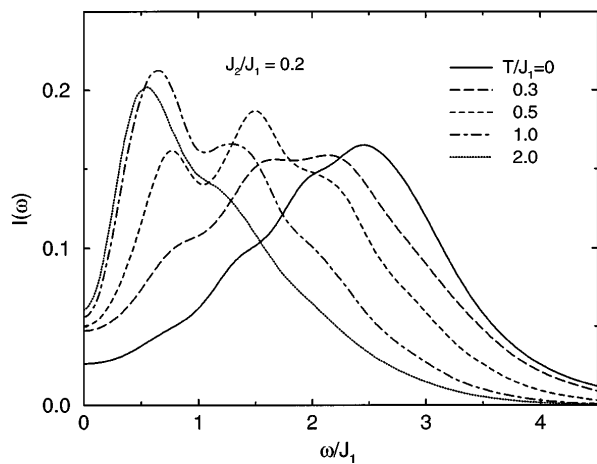
FIG. 4. I/A^2 vs ω/J for various T/J_1, as calculated at fixed $J_2 = 0.2J_1$ and $N = 20$. The smoothening is $\Delta = 0.4J_1$ for $T/J_1 \leq 0.3$ and $\Delta \leq 0.2J_1$ for $T/J_1 \geq 0.5$.

two-magnon-like peak with the maximum at $\omega^* \sim 2.5J_1$ gradually disappears with increasing T. At $T \gtrsim J_1$ it is substituted by a spectra peaked at much lower $\omega < J_1$. It should be noted that this development is quite different from the 2D Heisenberg model where the relatively narrow two-magnon peak at $T \sim 0$ mainly broadens with increasing $T \gtrsim J$, with only a small reduction in $\langle \omega \rangle$ [12]. Another interesting feature in Fig. 4 is the persistence of the pseudogap at low $\omega < 0.5J_1$, even at $T \gg J_1$ (clearly not present for the 2D Heisenberg model [12]). This gap is most pronounced for $J_2 = 0$, where it seems that at any T we have $I(\omega \to 0) = 0$, while it gradually fills up with adding $J_2 \neq 0$. It is possible that this phenomenon is related to the integrability of the 1D Heisenberg model (with $J_2 = 0$), since similar effects have been recently found in certain response functions within integrable models [18]. Some features of this spectra, such as low-frequency peaks and sharpening of spectral features with temperature, are rather similar to experiments. However, the experiments show a quasielastic peak at high temperatures and this is not seen in our numerical data. The extent to which these discrepancies are related to closeness to an integrable model on the theoretical side and lack of true-one dimensionality on the experimental side, needs to be further investigated.

Our main findings are that the low-temperature spectra are broad and occur at high energies in the power-law Néel phase and become narrower and move to lower energies in the spontaneously dimerized phase. They diminish in intensity with increase in temperature. At higher temperatures we reproduce the experimental finding that with increasing temperature the spectral features shift to lower frequencies, leading to much narrower central-peak form. However, unlike the experiments, where the peak becomes quasielastic and intensity continues to increase with T (which could be an indication of some additional

mechanism at very high T), in our studies the spectra at high-T remain of finite width and intensity, with a narrow pseudogap persisting at low frequencies. This could be related to the integrability of the 1D Heisenberg model with purely nearest-neighbor interactions, introducing an interesting theoretical issue but possibly not directly related to experiments. Comparison with the experimental spectra shows that the nearest-neighbor model does not account for the properties of $CuGeO_3$. If we take $J = 80$ K then the experimental spectra are peaked above $4J$. However, this is inconsistent with our calculations. On the other hand, well into the spontaneously dimerized phase the theoretical spectra are peaked below J_1, which is also inconsistent with experiments. On the other hand, with J_1 near 150 K, the spectra are peaked near frequency $2J_1$ and this is as calculated for J_2 near 0.2. These findings are consistent with previous theoretical studies of these systems by Castilla *et al.* [5].

[1] M. Hase, I. Terasaki, and K. Uchinokura, Phys. Rev. Lett. **70**, 3651 (1993).
[2] M. Nishi, O. Fujita, and J. Akimitsu, Phys. Rev. B **50**, 6508 (1994).
[3] K. Hirota *et al.,* Phys. Rev. Lett. **73**, 736 (1994).
[4] J. Riera and A. Dorby, Phys. Rev. B **51**, 16 098 (1995).
[5] G. Castilla, S. Chakravarty, and V. J. Emery, Phys. Rev. Lett. **75**, 1823 (1995).
[6] C. K. Majumdar and D. K. Ghosh, J. Math. Phys. (N.Y.) **10**, 1388, 1399 (1969).
[7] P. H. M. van Loosdrecht *et al.,* Phys. Rev. Lett. **76**, 311 (1996).
[8] P. Lemmens *et al.* (to be published); V. N. Muthukumar *et al.* (to be published).
[9] P. Fleury and R. Loudon, Phys. Rev. **166**, 514 (1968); J. B. Parkinson, J. Phys. C **2**, 2012 (1969).
[10] B. S. Shastry and B. I. Shraiman, Phys. Rev. Lett. **65**, 1068 (1990).
[11] J. Jaklič and P. Prelovšek, Phys. Rev. B **49**, 5065 (1994); *ibid.* **50**, 7129 (1994); Phys. Rev. Lett. **74**, 3411 (1995).
[12] P. Prelovšek and J. Jaklič, Phys. Rev. B **53**, 15 095 (1996).
[13] S. N. Coppersmith (unpublished); T. C. Hsu, Phys. Rev. B **41**, 11 379 (1990).
[14] J. B. Parkinson, J. Phys. C **2**, 2012 (1969).
[15] G. Müller, H. Beck, and J. C. Bonner, Phys. Rev. Lett. **43**, 75 (1979); G. Müller, H. Thomas, H. Beck, and J. C. Bonner, Phys. Rev. B **24**, 1429 (1981).
[16] B. S. Shastry and D. Sen, Report No. SISSA cond-mat/9603179.
[17] B. S. Shastry and B. Sutherland, Phys. Rev. Lett. **47**, 964 (1981).
[18] X. Zotos and P. Prelovšek, Phys. Rev. B **53**, 983 (1996).